FEBS Letters 589 (2015) 1399–1405

journal homepage: www.FEBSLetters.org

Biosensor-based affinities and binding kinetics of small molecule antagonists to the adenosine A_{2A} receptor reconstituted in HDL like particles

Elena Segala, James C. Errey, Cédric Fiez-Vandal, Andrei Zhukov, Robert M. Cooke *

Heptares Therapeutics, Biopark, Welwyn Garden City, Hertfordshire AL7 3AX, UK

ARTICLE INFO

Article history:
Received 24 February 2015
Revised 14 April 2015
Accepted 17 April 2015
Available online 29 April 2015

Edited by Christian Griesinger

Keywords:
Surface plasmon resonance
G protein-coupled receptor
Residence time
Lipid disc

ABSTRACT

The options for investigating solubilised G protein-coupled receptors (GPCRs) by biophysical techniques have long been hampered by their instability. A thermostabilised adenosine A_{2A} receptor expressed in insect cells, purified in detergent and reconstituted into high-density lipoprotein (HDL) particles was immobilised onto a Surface Plasmon Resonance sensor chip. This allowed measurement of affinities and kinetics for A_{2A} antagonists with affinities ranging from 50 pM to almost 2 μM. Compared with other formats, reproduction of affinities, and dissociation and association rate constants are good, reasonable and poor respectively, indicating stabilised receptors in HDL particles are useful for investigating specific aspects of GPCR-ligand interactions.

1. Introduction

G protein-coupled receptors (GPCRs) are the targets of around 30–40% of all marketed drugs [1]. However, many approaches successfully applied to drug discovery for soluble proteins [2] have had limited impact on GPCR targets, primarily due to the difficulty in obtaining pure, active, membrane-free receptors for structural and biophysical investigations. Recent developments in protein engineering and handling have led to crystallisation and structure determination for more than 20 GPCRs [3–5], with one technique, conformational thermostabilisation [6], also allowing the generation of solubilised GPCRs for investigation by multiple biophysical techniques. One of these, Surface Plasmon Resonance (SPR), is label-free and requires only a few micrograms of protein to generate binding affinity and kinetics data in real time. SPR has been used with detergent solubilised GPCRs for Biophysical Mapping of ligand binding sites [7], screening of fragment libraries [8] and kinetic profiling of compounds [9].

While detergent solubilised GPCRs have been extremely useful for studying ligand binding, it is now possible to produce membrane proteins in reconstituted high-density lipoprotein (rHDL) particles. rHDLs are self-assembled discoidal fragments of nanolipid bilayers that are stabilised in solution by amphipathic helical scaffold proteins. They are stable and highly soluble membrane mimetics with controlled lipid composition. A broad range of membrane proteins have already proven to remain monodisperse and active after reconstitution into such native-like bilayer particles [10,11]. However, only four have been so far self-assembled into rHDLs for the purpose of SPR studies: the tissue factor (TF) [12], the glycolipid receptor G_{M1} [13], the CD4 receptor [14] and the neurotensin receptor type 1 [15]. All of these investigations were limited to protein–protein interactions and to date, there is no work describing the use of rHDLs for determining binding kinetics of small ligands to membrane proteins.

The receptor residence time [16] has developed into an important consideration in drug discovery. Particularly with rapid metabolic clearance, the residence time on the target receptor may be more important than the affinity in determining a

Abbreviations: DDM, n-dodecyl-β-D-maltoside; DM, decyl-β-D-maltopyranoside; GPCR, G protein-coupled receptor; NTA, nitrilotriacetic acid; PhT, phenol triazine; POPC, 1-palmitoyl-2-oleoyl-*sn*-glycero-3-phosphocholine; POPG, 1-palmitoyl-2-oleoyl-*sn*-glycero-3-phosphoglycerol; rHDL, reconstituted high-density lipoprotein; RU, resonance unit; SPA, scintillation proximity assay; SPR, Surface Plasmon Resonance; StaR, stabilised receptor; XAC, xanthine amine congener

Author contributions: Participated in research design: Segala, Errey, Fiez-Vandal, Cooke. Conducted experiments: Segala, Zhukov. Performed data analysis: Segala, Fiez-Vandal, Cooke. Wrote or contributed to the writing of the manuscript: Segala, Zhukov, Fiez-Vandal, Cooke.

* Corresponding author at: Heptares Therapeutics, Biopark, Broadwater Road, Welwyn Garden City, Hertfordshire AL7 3AX, UK. Fax: +44 1707358640.

E-mail address: rob.cooke@heptares.com (R.M. Cooke).

http://dx.doi.org/10.1016/j.febslet.2015.04.030
0014-5793/

pharmacodynamic effect [17]. Hence determination of the kinetics of ligand binding, specifically the dissociation rate, is of growing interest. In this study, we use SPR to examine the affinities and binding kinetics of ligands to the adenosine A_{2A} receptor ($A_{2A}R$), which is the focus of drug discovery efforts for poorly addressed neurological disorders such as Parkinson's disease. The A_{2A} receptor has been thermostabilised in the presence of an antagonist [6], resulting in a receptor, A_{2A}-StaR2, which maintains binding affinity for antagonists while having reduced binding for agonists. The A_{2A}-StaR2 was reconstituted in rHDLs and immobilised on an SPR sensor chip to determine the affinities and association/dissociation kinetics of antagonists spanning an almost 36000 fold range in affinity. Our results show that using stabilised receptors, SPR and rHDLs represents a new opportunity to obtain affinities and kinetics from low molecular weight compounds binding to GPCRs.

2. Materials and methods

2.1. Compounds

SLV320, KW3902, DPCPX, xanthine amine congener (XAC), SCH58261, SCH442416 and ZM241385 are from Tocris Bioscience, UK. CGS15943 and theophylline are from Sigma–Aldrich, UK. 4-(3-amino-5-phenyl-1,2,4-triazin-6-yl)-2-chlorophenol (compound 4e from Congreve et al. [18]) is produced by Heptares Therapeutics

Table 1
Kinetic characterisation of a set of 9 adenosine antagonists using SPR on A_{2A}-StaR2 solubilised in DDM micelles or A_{2A}-StaR2 in rHDLs. The assay was conducted at 10 °C in a multi-cycle format or a single-cycle format depending on the kinetic parameters of the ligand. The range of concentrations used for the ligand is indicated in the right-hand side column. For theophylline a saturation binding curve is also shown. In addition to the experimental traces the fit calculated by the Biacore software is also displayed.

Compound	A_{2A}-StaR2 in DDM micelles	A_{2A}-StaR2 in rHDLs	Concentration (nM)
Theophylline  180 Da	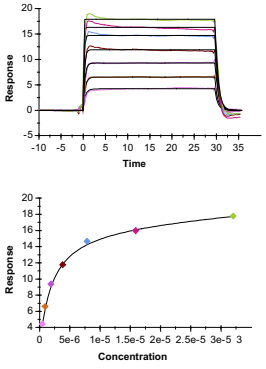	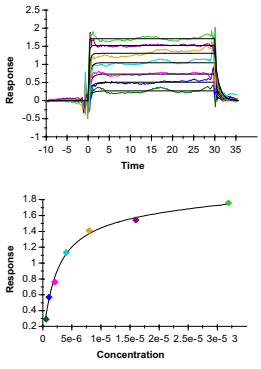	500 (lowest trace) 1000 2000 4000 8000 16000 32000 (top trace)
SLV320 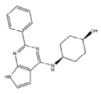 308 Da	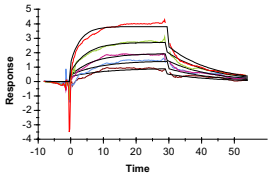	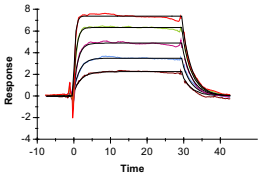	125 (lowest trace) 250 500 1000 2000 (top trace)
DPCPX 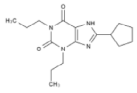 304 Da	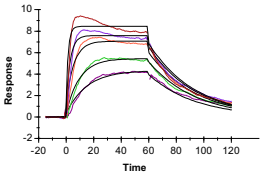	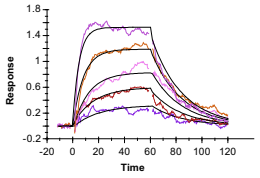	6.25 (lowest trace) 12.5 25 50 100 (top trace)
KW3902 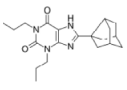 356 Da	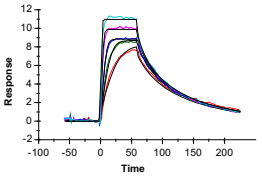	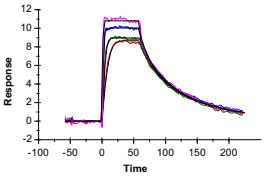	62.5 (lowest trace) 125 250 500 1000 (top trace)

(*continued on next page*)

Table 1 (*continued*)

XAC 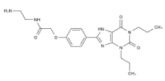 465 Da	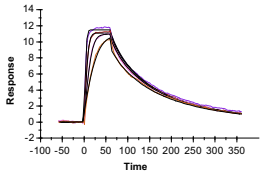	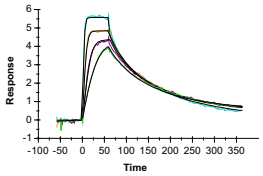	50 (lowest trace) 100 200 400 800 (top trace)
SCH58261 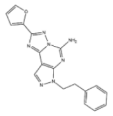 345 Da	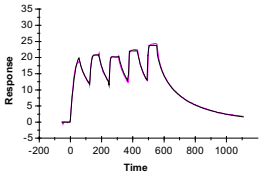	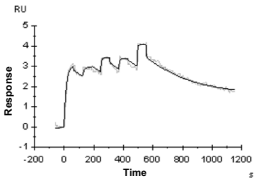	6.25 (first injection) 12.5 25 50 100 (last injection)
ZM241385 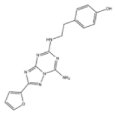 337 Da	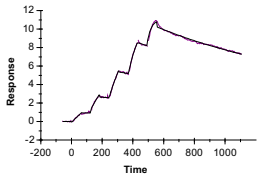	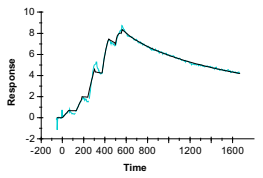	1.56 (first injection) 3.13 6.25 12.5 25 (last injection)
SCH442416 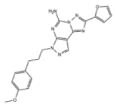 389 Da	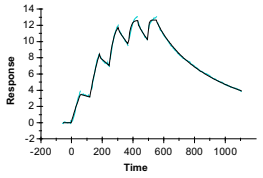	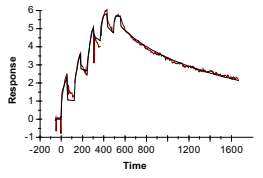	12.5 (first injection) 25 50 100 200 (last injection)
Phenol triazine 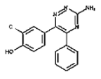 299 Da	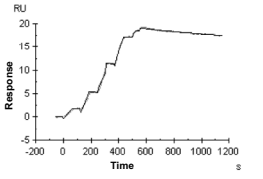	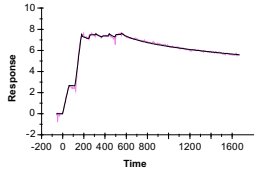	6.25 (first injection) 12.5 25 50 100 (last injection)

and is referred to here as a phenol triazine (PhT). [^{3}H]ZM241385 is from American Radiolabeled Chemicals (50 Ci/mmol).

2.2. Protein engineering

The human adenosine A_{2A}-StaR2 used in this work was stabilised in the presence of an inverse agonist (ZM241385) [6]. It has 8 thermostabilising mutations compared to the wild-type receptor: A54L, T88A, K122A, N154A, V239A, R107A, L235A and S277A. The first three amino acids are deleted and the protein has a C-terminal truncation after K315. A deca-histidine tag has been added at the C-terminus.

The zebrafish apolipoprotein A-I (Zap1) [19] has a PreScission protease site followed by a hexa-histidine tag at the C-terminus.

2.3. Expression and purification

The adenosine A_{2A}-StaR2 was expressed using the baculovirus system. Tni PRO cells were grown in ESF921 medium (Expression Systems) supplemented with 5% (v/v) foetal bovine serum (Sigma–Aldrich) and 1% (v/v) penicillin and streptomycin. Cells were infected at a density of 2.6 million cells per ml with recombinant virus at an approximate multiplicity of infection (MOI) of 1. Cells were harvested by centrifugation 48 h post-infection.

Membranes were prepared from a one litre cell pellet resuspended in 40 mM Tris–HCl pH 7.6, 1 mM EDTA, Complete EDTA free protease inhibitor cocktail tablets (Roche). Cells were disrupted by a single passage through a microfluidizer (processor M-110L Pneumatic, Microfuidics) cooled with ice (lysis pressure

Table 2
The equilibrium dissociation constant, and association and dissociation rate constants for the A_{2A}-StaR2 when detergent solubilised, in rHDLs and in membranes. k_a is expressed in 1/Ms, k_d in 1/s and residence time ($1/k_d$) in min. All pK_i values from the literature are for the wild type A_{2A} receptor, except for PhT (A_{2A}-StaR2).

		Biacore A_{2A}-StaR2 in DDM micelles	Biacore A_{2A}-StaR2 in rHDLs	Radioligand binding assay membranes	Literature
Theophylline	Kinetic pK_D	5.71	5.78		
	Competition pK_i			6.28	5.74[22]
SLV320	k_a	1.3×10^5	9.9×10^5	$1.82 \pm 0.8 \times 10^4$	
	k_d	7.6×10^{-2}	3.8×10^{-1}	$3.58 \pm 1.6 \times 10^{-2}$	
	Kinetic pK_D	6.23	6.42	5.70	
	Competition pK_i			6.38	6.40[23]
	Residence time	0.22	0.04	0.47	
DPCPX	k_a	$4.8 \pm 0.6 \times 10^5$	$4.5 \pm 0.9 \times 10^5$	$5.10 \pm 1.5 \times 10^4$	
	k_d	$3.5 \pm 0.6 \times 10^{-2}$	$4.4 \pm 0.5 \times 10^{-2}$	$7.66 \pm 1.0 \times 10^{-3}$	
	Kinetic pK_D	7.12	6.95	6.81	
	Competition pK_i			7.64	6.89[24] 6.63[25]
	Residence time	0.48	0.37	2.18	
KW3902	k_a	$4.5 \pm 0.4 \times 10^5$	$2.2 \pm 0.9 \times 10^5$	$4.88 \pm 0.4 \times 10^5$	
	k_d	$1.5 \pm 0.2 \times 10^{-2}$	$2.4 \pm 0.8 \times 10^{-2}$	$1.69 \pm 0.4 \times 10^{-2}$	
	Kinetic pK_D	7.46	6.89	7.47	
	Competition pK_i			7.99	6.97[26]
	Residence time	1.10	0.69	0.99	
XAC	k_a	$1.2 \pm 0.2 \times 10^6$	$9.2 \pm 2 \times 10^5$	$2.60 \pm 0.1 \times 10^5$	
	k_d	$2.6 \pm 0.5 \times 10^{-2}$	$1.7 \pm 0.3 \times 10^{-2}$	$2.63 \pm 0.2 \times 10^{-3}$	
	Kinetic pK_D	7.68	7.74	7.95	
	Competition pK_i			8.47	9.00[24] 8.05[25]
	Residence time	0.65	1.01	6.34	
SCH58261	k_a	$3.5 \pm 0.5 \times 10^6$	$3.6 \pm 2.8 \times 10^6$	$2.13 \pm 0.4 \times 10^6$	
	k_d	$2.3 \pm 0.2 \times 10^{-2}$	$8.9 \pm 4.2 \times 10^{-3}$	$7.62 \pm 1.2 \times 10^{-3}$	
	Kinetic pK_D	8.19	8.40	8.45	
	Competition pK_i			8.55	9.22[24] 8.96[25]
	Residence time	0.74	1.87	2.19	
ZM241385	k_a	$2.0 \pm 0.2 \times 10^6$	$3.0 \pm 0.7 \times 10^6$	$6.58 \pm 2.7 \times 10^6$	
	k_d	$7.9 \pm 0.6 \times 10^{-4}$	$7.5 \pm 1.2 \times 10^{-4}$	$3.89 \pm 0.1 \times 10^{-3}$	
	Kinetic pK_D	9.40	9.49	9.18	
	Competition pK_i			9.19	9.40[27] 9.10[24]
	Residence time	21.14	22.09	4.28	
SCH442416	k_a	$7.9 \pm 1.4 \times 10^5$	$7.3 \pm 1.3 \times 10^5$	$3.70 \pm 1.2 \times 10^6$	
	k_d	$3.3 \pm 0.2 \times 10^{-3}$	$1.3 \pm 0.1 \times 10^{-3}$	$6.92 \pm 0.5 \times 10^{-3}$	
	Kinetic pK_D	8.33	8.69	8.74	
	Competition pK_i			8.92	10.3[28]
	Residence time	4.98	12.63	2.41	
PhT	k_a	$8.7 \pm 0.7 \times 10^5$	$1.2 \pm 0.7 \times 10^7$	$2.74 \pm 0.6 \times 10^6$	
	k_d	$1.5 \pm 0.1 \times 10^{-4}$	$5.8 \pm 4 \times 10^{-4}$	$2.06 \pm 0.1 \times 10^{-3}$	
	Kinetic pK_D	9.74	10.38	9.11	
	Competition pK_i			9.74	8.85[18]
	Residence time	108.70	28.97	8.11	

~15 000 psi) and membranes were pelleted by ultracentrifugation at 204 700×*g* and stored at −80 °C. Membranes were solubilised with 2% n-decyl-β-D-maltopyranoside (DM) for 1 h at 4 °C followed by ultracentrifugation to remove insoluble material.

The solubilised material was applied to a 5 ml Ni–NTA (nickel–nitrilotriacetic acid) superflow cartridge (Qiagen) and the protein eluted with 40 mM Tris–HCl pH 7.4, 400 mM NaCl, 0.15% DM, 280 mM imidazole and 3 mM theophylline. Elution fractions containing the 36 kDa protein were pooled and concentrated. The protein sample was applied to a Superdex 200 10/300 GL size exclusion column (GE Healthcare). The final protein concentration was determined using a detergent compatible Bradford assay (Bio-Rad) and quantitative amino-acid analysis.

Throughout purification the concentration of functional, purified receptor was determined by scintillation proximity assay (SPA) with a 20 nM concentration of [^{3}H]ZM241385 (40× over K_D) saturating completely the receptor.

Zebrafish apolipoprotein A-I (Zap1) was expressed in *Escherichia coli* by using a pET28a vector and purified as previously described [19].

2.4. Reconstitution into rHDLs

The purified A_{2A}-StaR2 (*ca.* 0.5 mg) was reconstituted into rHDLs as previously described [19] using Zap1 as a scaffold protein and the following lipids: 1-palmitoyl-2-oleoyl-*sn*-glycero-3-phosphocholine (POPC), 1-palmitoyl-2-oleoyl-*sn*-glycero-3-phosphoglycerol (POPG) and cholesterol (CHO) in a 3:2:0.5 molar ratio (Avanti Polar Lipids). The Zap1:lipid ratio was kept around 1:100 and the ratio of A_{2A}R:Zap1 was 1:2.5.

Receptor, phospholipids and scaffold protein were incubated at 4 °C for 1 h with rolling agitation before Bio-Beads SM-2 (Bio-Rad) were added (1 g of beads per ml) to remove the detergent and initiate disc self-assembly. After overnight incubation at 4 °C with

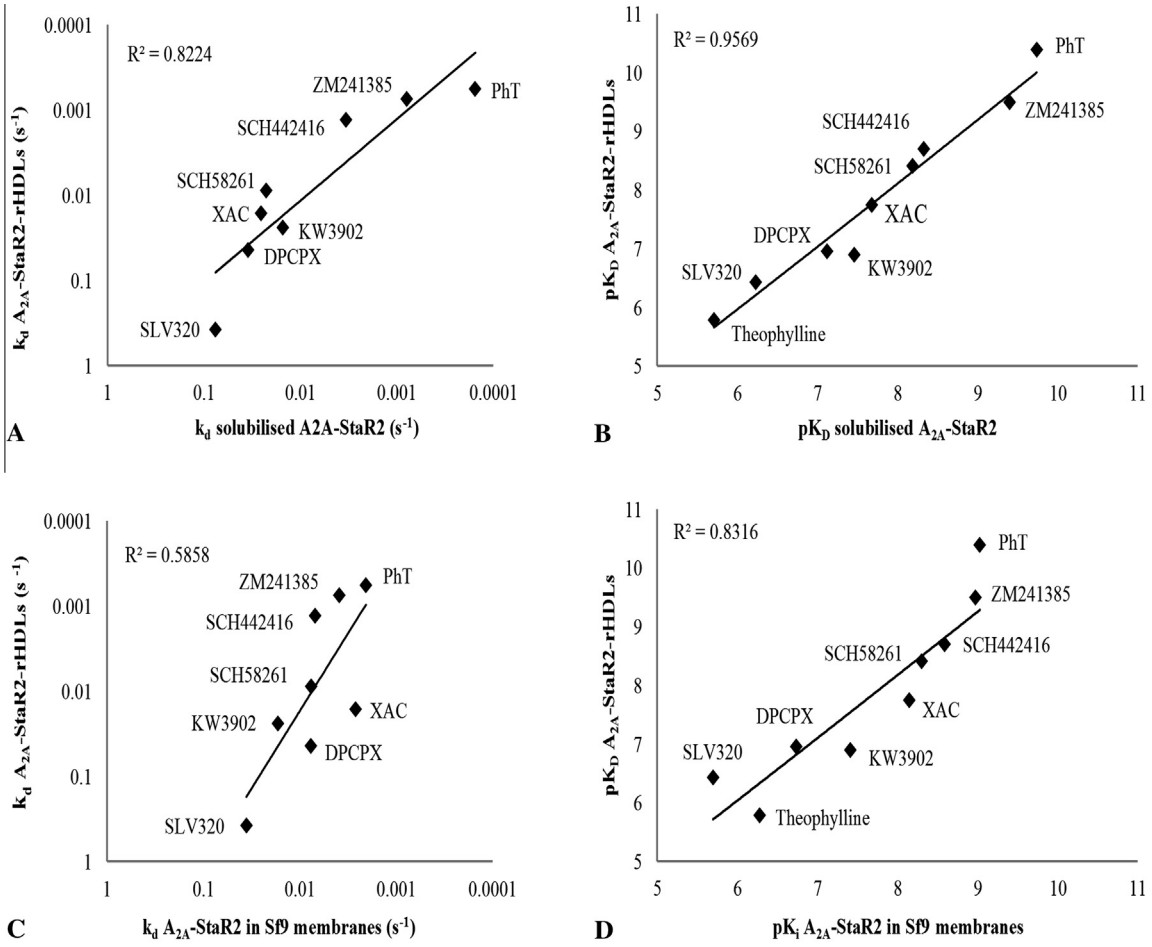

Fig. 1. (A and B) Plots of k_d and pK_D values, respectively, of A_{2A}-StaR2 in detergent micelles and A_{2A}-StaR2 in rHDLs. (C and D) Plots of k_d and pK_D/pK_i, respectively, of A_{2A}-StaR2 in cell membranes and A_{2A}-StaR2 in rHDLs.

agitation, the hexa-histidine tag of Zap1 was cleaved by adding 0.5 mM DTT and 1 µl of PreScission Protease (GE Healthcare) and incubating for 1 h at room temperature, leaving the histidine tag on the receptor to bind the NTA sensor chip.

A_{2A}R-StaR2 rHDLs were separated from aggregated material and empty discs by gel filtration onto a Superdex 200 10/300 GL column (GE Healthcare) with 10 mM HEPES pH 7.5, 100 mM NaCl. Fractions containing the assembled rHDLs were pooled and concentrated. Final concentration was measured by a BCA assay and the specific activity (pmol/mg) of the reconstituted receptor was measured by SPA.

2.5. Radioligand binding

SPA binding reactions were performed in 200 µl final volume in buffer containing 20 mM HEPES pH 7.4, 1 mM $MgCl_2$, 0.1% BSA, and 0.15% DM when assays were performed on solubilised receptors. [^{3}H]ZM241385 (20 nM) was added to copper-chelate YSi scintillation SPA beads (150 µg/well, PerkinElmer). 10 ng, 50 ng or 100 ng of solubilised A_{2A}-StaR2 or reconstituted A_{2A}-StaR2 was added per well. Non-specific binding was determined in the presence of 10 µM unlabelled ZM241385. The plate was shaken on a vibrating platform for 1 h at room temperature before counting on a MicroBeta liquid scintillation counter (SPA cpm mode, Wallac).

For filtration assays, cell membranes from Sf9 cells expressing the A_{2A}-StaR2 were incubated in buffer containing 50 mM Tris–HCl pH 7.4 with [^{3}H]ZM241385 in a total assay volume of 1 ml with a final DMSO concentration of 1%. Assays were performed as previously described [6]. K_D values were obtained using a global fitted one-site binding hyperbola in Prism 5.04 (GraphPad, San Diego, CA, USA).

Competition binding was performed by incubating membranes (10 µg/well) with [^{3}H]ZM241385 (1.5 nM) and a range of test antagonist concentrations (from 10^{-4} to 10^{-12} M). Association and dissociation data were fitted globally in Prism 5.04 to determine IC_{50} values. These were converted to K_i values using the Cheng–Prusoff equation $K_i = IC_{50}/(1 + [L]/K_D)$.

Association kinetic parameters for [^{3}H]ZM241385 were determined by adding the same cell membranes (10 µg protein/well) and 0.1, 0.3 or 0.9 nM radioligand at time points of 0, 20, 40, 48, 52, 56, 58, 59, 59.5 and 60 min. Dissociation kinetic parameters were determined by pre-equilibrating membranes and [^{3}H]ZM241385 for 1 h; a saturating concentration of unlabelled CGS15943 (1 µM) was then added at the same time points as above. Kinetics of binding of unlabelled compounds were determined using the method of Motulsky and Mahan [20]. Association curves for [^{3}H]ZM241385 were determined in the absence or presence of three concentrations of competitive antagonist (typically 0.3, 1 and $3 \times K_D$ value). Association and dissociation rate constants for unlabelled compounds were calculated by global analysis of the association data sets, as previously described [21]. Ligand-receptor residence times were calculated as $1/k_d$.

All assays were conducted twice in triplicate.

2.6. Surface Plasmon Resonance experiments

SPR analyses were carried out at 10 °C on a Biacore T200 instrument using NTA sensor chips (GE Healthcare) with a flow rate of 30 μl/min. The running buffer was PBS with 0.05 mM EDTA and 5% DMSO. 0.1% n-dodecyl-β-D-maltoside (DDM) was added for experiments with the solubilised receptor.

Ligands were prepared over a double-dilution series (5 concentrations) and injected in either a multi- or a single-cycle format depending on their kinetic parameters. The actual concentrations as well as contact and dissociation times varied between the ligands depending on the kinetics and affinity of interaction. The data were fitted to a 1:1 interaction model using the kinetics evaluation software from Biacore. A minimum of three measurements were recorded for each interaction. All calculations of correlation coefficients are on a logarithmic basis, *i.e.* using pk_a, pk_d, pK_D and pK_i.

3. Results

3.1. Purification of A_{2A}-StaR2 and reconstitution into rHDLs

The C-terminally His_{10}-tagged A_{2A}-StaR2 receptor was purified to near homogeneity through a single step of metal chelate affinity chromatography. During purification, theophylline, a low affinity ligand (K_D ~2 μM) provided additional stability to the receptor. 0.5 mg of receptor was reconstituted into rHDLs using Zap1 in a 1:2.5 A_{2A}R to scaffold protein ratio. The final yield of A_{2A}R and Zap1 was 220 μg. As the A_{2A}R is approximately half of the disc complex, approximately 20% of the initial purified receptor has been reconstituted into rHDLs. Copper-chelate SPA assays showed that both solubilised and reconstituted receptors bound [^{3}H]ZM241385 with high Bmax values, 97% and 92% of active receptor fractions, respectively.

3.2. SPR experiments on A_{2A}-StaR2

To compare the pharmacology of A_{2A}-StaR2 in rHDLs with that of the receptor in detergent micelles, 9 antagonists were tested by SPR. These ligands have molecular weights ranging from 180 Da (theophylline) to 464 Da (XAC) and reported affinities for the wild-type A_{2A} receptor from 50 pM (SCH442416) to 1.8 μM (theophylline) [18,22–28].

The A_{2A}-StaR2 in DDM micelles and in rHDL bilayers were successfully immobilised on the Biacore sensor chip, with a slightly lower increase observed for the A_{2A}-StaR2-rHDLs (increase by 5000–7000 resonance units, RU) compared to the solubilised receptor (increase by 10000–12000 RU). Both samples gave measurable amplitudes for all compounds tested.

Concentration response experiments for A_{2A}-StaR2 in DDM micelles and rHDL bilayers are shown for the compounds tested in Table 1. The sensorgrams are quite different between compounds, requiring a move from multi-cycle to single-cycle experiments for those of higher affinity. The concentration response experiments provided affinities and association and dissociation rate constants for all of the ligands tested except theophylline (Table 2). For this ligand, SPR data approach saturation for both forms of the receptor and affinities can be calculated; however, the association and dissociation rates were too fast to allow measurement of rate constants with confidence. The correlation between the association rate constants measured for A_{2A}-StaR2 in DDM micelles and in rHDL bilayers is poor (R^2 = 0.23, data not shown), whereas the correlations between these two forms of the receptor for the dissociation rate constants (R^2 = 0.82) and the affinities (R^2 = 0.96) are very good (Fig. 1A and B).

3.3. Radioligand binding experiments on A_{2A}-StaR2 in cell membranes

In addition to the SPR experiments on the A_{2A}-StaR2 in DDM micelles and in rHDLs, radioligand binding studies were performed on the receptor expressed in Sf9 insect cells. The saturation and kinetically-derived pK_D values for [^{3}H]ZM241385 (9.19 and 9.18, respectively) for A_{2A}-StaR2 in cell membranes are in good agreement with the pK_D values measured by SPR for the solubilised receptor (9.40) and the receptor in rHDLs (9.49). The association and dissociation rate constants of [^{3}H]ZM241385 are also close to the values obtained by SPR for the unlabelled ZM241385 (Table 2).

Unlabelled adenosine receptor antagonists were tested in competition binding experiments against [^{3}H]ZM241385, and pK_i values are reported in Table 1. XAC, SCH58261, ZM241385, SCH442416 and PhT show high affinity binding to A_{2A}-StaR2 in membranes, with pK_i values close to the published ones for the wild-type receptor, whereas theophylline, SLV320, DPCPX and KW3902 have affinities between 10 nM and 2 μM, also in agreement with literature data.

Variations in the association and dissociation rate constants are observed when comparing data from SPR experiments with those from radioligand binding experiments (Table 2). The correlation between association rate constants for A_{2A}-StaR2 in detergent and in membranes is reasonable (R^2 = 0.59, data not shown), while correlation between A_{2A}-StaR2 in rHDLs and in membranes is poor (R^2 = 0.26, data not shown). The correlations between the dissociation rate constants are reasonable, for receptors in membranes and DDM micelles (R^2 = 0.46) and for receptors in membranes and rHDLs (R^2 = 0.59) (Fig. 1C). The pK_D values generated by SPR correlate well with pK_i values from radioligand binding experiments in membranes (R^2 = 0.89 between receptors in membranes and detergent; R^2 = 0.83 between receptors in membranes and rHDLs) (Fig. 1D).

The pK_D values generated by SPR are also comparable with the published pK_i values from competitive radioligand binding experiments of the wild-type A_{2A} receptor in cell membranes or native tissue (Table 2).

4. Discussion

There is mounting evidence to suggest that binding kinetics can influence the efficacy of a drug [16,17], hence there is often a desire to rank compounds by their dissociation kinetics prior to selecting a development candidate. Although previous data [7,29] from a stabilised adenosine A_{2A} receptor solubilised and immobilised on a biosensor chip support its use for profiling compound binding affinities and kinetics, there are circumstances where this format may not be ideal. Ligands with poor solubility and high *clog P* can partition within micelles [30], reducing the effective concentration and distorting estimation of affinities and kinetics. Additionally, detergents do not provide the same lateral pressure and charge distribution as a lipidic leaflet and could disrupt high affinity binding [19,31]. Third, detergents interfere with binding of additional components such as G proteins [15,32].

To explore a format which could address these concerns, A_{2A}-StaR2 was reconstituted into rHDLs and tested by SPR with the same set of antagonists as the solubilised receptor. The higher molecular weight of the GPCR-rHDL complex (approximately 160 to 180 kDa) vs A_{2A}-StaR2 micelles (approximately 100 kDa) reduces the number of receptors immobilised on the chip, increasing the need for a high proportion of receptors able to bind ligands to obtain usable sensorgrams (Table 1). This favours the use of stabilised receptors which allow high fractions of active receptor to be maintained during purification and reconstitution.

Replacing the detergent with rHDLs containing phospholipids and cholesterol maintained the affinities and dissociation rates for the A_{2A}-StaR2 antagonists (Table 1 and Fig. 1). As for the solubilised receptor, SPR affinities and dissociation rates are in line with those published in the literature and obtained by competitive radioligand binding kinetics.

In this study correlations between compounds measured in different formats are generally very good for affinities, reasonable for dissociation rate constants, and poor for association rate constants. The very good correlation for affinities gives us confidence that SPR can be used with stabilised GPCRs reconstituted into rHDLs as well as solubilised in detergent for profiling ligands. There is no loss in binding affinity for the stabilised receptor whereas wild-type GPCRs often show rightward shifts to lower affinities after detergent solubilisation [11,19,31]. The fact that the worst correlations are for association rate constants is not surprising, as their calculation directly depends on knowledge of the ligand concentration, which may be subject to unaccounted errors, such as from insolubility or partitioning. The reasonable correlation of dissociation rate constants would be sufficient to support lead optimisation where the major use is expected to be ranking of compounds based on relative rates. As the residence times are derived from the dissociation rate constants, equivalent trends are observed. In each case DPCPX has the shortest residence time and PhT the longest, but the range varies considerably (from 0.22 to 108 min for the A_{2A}-StaR2 in DDM micelles, to 0.04 to 29 min for the rHDL discs, to 0.47 to 8.1 min for the membranes). Hence while these can be used to compare compounds, it remains to be established which format is closest to an *in vivo* situation.

In conclusion, using a thermostabilised adenosine A_{2A} receptor, we have shown that the immobilisation of a receptor reconstituted into rHDLs on a sensor chip can provide useful affinities and binding kinetics data. As the SPR technique does not require competition with a labelled compound it is well suited to monitor binding at a range of sites, such as those of allosteric modulators. This is the first time the measurement of ligand affinities and binding kinetics has been achieved by SPR on a rHDL-reconstituted GPCR in the absence of radio- or fluorescently labelled tracer molecules. This is a new approach to characterise the interactions between small molecules and GPCRs and it provides another means for using binding kinetics during compound optimisation. The data presented here do not clearly indicate whether the detergent micelles or rHDLs are the superior format. Rather, both are reliable, and it is more likely that the choice of format may depend on the system to be studied, with detergent micelles easier to produce and giving higher sensitivity, and rHDLs offering a more native-like environment and avoiding problems of ligands partitioning into micelles. In addition the rHDL format allows the binding of ligands to GPCRs to be studied in the presence of other components, such as G proteins.

Acknowledgements

The authors thank Richard Mould for advice on competitive radioligand binding kinetics.

The research leading to these results has received support from the Innovative Medicines Initiative Joint Undertaking under K4DD, grant agreement no. 115366, resources of which are composed of financial contribution from the European Union's Seventh Framework Programme (FP7/2007-2013) and EFPIA companies' in kind contribution. More info: www.imi.europa.eu.

References

[1] Rask-Andersen, M. (2010) Trends in the exploitation of novel drug targets. Nat. Rev. Drug Discov. 10, 579–590.
[2] Alex, A.A. and Millan, D.S. (2012) Contribution of structure-based drug design to the discovery of marketed drugs. RSC Drug Discov. Ser. 13.
[3] Doré, A.S., Okrasa, K., Patel, J.C., et al. (2014) Structure of class C GPCR metabotropic glutamate receptor 5 transmembrane domain. Nature 511, 557–562.
[4] Srivastava, A., Yano, J., Hirozane, Y., et al. (2014) High-resolution structure of the human GPR40 receptor bound to allosteric agonist TAK-875. Nature 513, 124–127.
[5] Wu, H., Wang, C., Gregory, K.J., et al. (2014) Structure of a class C GPCR metabotropic glutamate receptor 1 bound to an allosteric modulator. Science 344, 58–64.
[6] Robertson, N., Jazayeri, A., Errey, J., et al. (2011) The properties of stabilised G protein-coupled receptors (StaRs) and their use in drug discovery. Neuropharmacology 60, 36–44.
[7] Zhukov, A., Andrews, S.P., Errey, J.C., et al. (2011) Biophysical mapping of the adenosine A_{2A} receptor. J. Med. Chem. 54, 4312–4323.
[8] Christopher, J.A., Brown, J., Doré, A.S., et al. (2013) Biophysical fragment screening of the β1-adrenergic receptor: identification of high affinity arylpiperazine leads using structure-based drug design. J. Med. Chem. 56, 3446–3455.
[9] Aristotelous, T., Ahn, S., Shukla, A.K., et al. (2013) Discovery of β2 adrenergic receptor ligands using biosensor fragment screening of tagged wild-type receptor. ACS Med. Chem. Lett. 4, 1005–1010.
[10] Bayburt, T.H. and Sligar, S.G. (2010) Membrane protein assembly into Nanodiscs. FEBS Lett. 584, 1721–1727.
[11] Fiez-Vandal, C., Leder, L., Freuler, F., et al. (2012) HDL-like discs for assaying membrane proteins in drug discovery. Biophys. Chem. 165–166, 56–61.
[12] Shaw, A.W., Pureza, V.S., Sligar, S.G., et al. (2007) The local phospholipid environment modulates the activation of blood clotting. J. Biol. Chem. 9, 6556–6563.
[13] Borch, J., Torta, F., Sligar, S., et al. (2008) Nanodiscs for immobilization of lipid bilayers and membrane receptors: kinetic analysis of cholera toxin binding to a glycolipid receptor. Anal. Chem. 80, 6245–6252.
[14] Glück, J.M., Koenig, B.W. and Willbold, D. (2011) Nanodiscs allow the use of integral membrane proteins as analytes in surface plasmon resonance studies. Anal. Biochem. 408, 46–52.
[15] Adamson, R.J. and Watts, A. (2014) Kinetics of the early events of GPCR signalling. FEBS Lett. 588, 4701–4707.
[16] Copeland, R.A., Pompliano, D.L. and Meek, T.D. (2006) Drug–target residence time and its implications for lead optimization. Nat. Rev. Drug Discov. 5, 730–739.
[17] Lu, H. and Tonge, P.J. (2010) Drug–target residence time: critical information for lead optimization. Curr. Opin. Chem. Biol. 14, 467–474.
[18] Congreve, M., Andrews, A.P., Doré, A.S., et al. (2012) Discovery of 1,2,4-triazine derivatives as adenosine A_{2A} antagonist using structure based drug design. J. Med. Chem. 55, 1898–1903.
[19] Banerjee, S., Huber, T. and Sakmar, T.P. (2008) rapid incorporation of functional rhodopsin into nanoscale apolipoprotein bound bilayer (NABB) particles. J. Mol. Biol. 377, 1067–1081.
[20] Motulsky, H.J. and Mahan, L.C. (1984) The kinetics of competitive radioligand binding predicted by the law of mass action. Mol. Pharmacol. 25, 1–9.
[21] Dowling, M.R. and Charlton, S.J. (2006) Quantifying the association and dissociation rates of unlabelled antagonists at the muscarinic M3 receptor. Br. J. Pharmacol. 148, 927–937.
[22] Bennett, K.A., Tehan, B., Lebon, G., et al. (2013) Phamacology and structure of isolated conformations of the adenosine A_{2A} receptor define ligand efficacy. Mol. Pharmacol. 83, 949–958.
[23] Kalk, P., Eggert, B., Relle, K., et al. (2007) The adenosine A1 receptor antagonist SLV320 reduces myocardial fibrosis in rats with 5/6 nephrectomy without affecting blood pressure. Br. J. Pharmacol. 151, 1025–1032.
[24] Fredholm, B., Ijzerman, A.J., Jacobson, K.A., et al. (2001) International union of pharmacology. XXV. Nomenclature and classification of adenosine receptors. Pharmacol. Rev. 53. 557-552.
[25] Zocchi, C., Ongini, E., Ferrara, S., et al. (1996) Binding of the radioligand [3H]-SCH 58261, a new non-xanthine A2A adenosine receptor antagonist, to rat striatal membranes. Br. J. Pharmacol. 117, 1381–1386.
[26] Pfister, J.R., Belardinelli, L., Lee, G., et al. (1997) Synthesis and biological evaluation of the enantiomers of the potent and selective A1-adenosine antagonist 1,3-dipropyl-8-[2-(5,6-epoxynorbonyl)]-xanthine. J. Med. Chem. 40, 1773–1778.
[27] Guo, D., Xia, L., van Veldhoven, J.P.D., et al. (2014) Binding kinetics of ZM241385 derivatives at the human adenosine A_{2A} receptor. ChemMedChem 9, 752–761.
[28] Todde, S., Moresco, R.M., Simonelli, P., et al. (2000) Design, radiosynthesis, and biodistribution of a new potent and selective ligand for in vivo imaging of the adenosine A2A receptor system using positron emission tomography. J. Med. Chem. 43 (4359–4362), 27.
[29] Rich, R.L., Errey, J., Marshall, F., et al. (2011) Biacore analysis with stabilized G-protein-coupled receptors. Anal. Biochem. 409, 267–272.
[30] Früh, V., Zhou, Y., Chen, D., et al. (2010) Application of fragment-based drug discovery to membrane proteins: identification of ligands of the integral membrane enzyme DsbB. Chem. Biol. 17, 881–891.
[31] Kuszak, A.J., Pitchiaya, S., Anand, J.P., et al. (2009) Purification and functional reconstitution of monomeric mu-opioid receptors: allosteric modulation of agonist binding by Gi_2. J. Biol. Chem. 284, 26732–26741.
[32] Cerione, R.A. (1991) Reconstitution of receptor/GTP-binding protein interactions. Biochim. Biophys. Acta 1071, 473–501.